**OWJ5.pdf**

# Fully Reconfigurable Silicon Photonic Lattice Filters with Four Cascaded Unit Cells

S. Ibrahim[1], L. W. Luo[2], S.S. Djordjevic [1], C. B. Poitras[2], L. Zhou[1], N.K. Fontaine[1], B. Guan[1], S. Cheung[1], Z. Ding[1], K.Okamoto[1], M. Lipson[2], and S. J. B. Yoo[1]
[1]*Department of Electrical and Computer Engineering, University of California, Davis, CA 95616, USA*
*e-mail: sbyoo@ucdavis.edu*
[2]*Department of Electrical and Computer Engineering, Cornell University, Ithaca, NY 14853, USA*
*e-mail: lipson@ece.cornell.edu*

**Abstract**: We present a fully-reconfigurable CMOS-compatible silicon-photonic lattice-filter with four cascaded unit cells consisting of resonant rings and Mach-Zehnder interferometers. The measurements show high-quality filter responses including IIR and FIR filter characteristics matching theoretical predictions.

**Introduction**:

All-optical signal processing can reduce the power consumption and bandwidth limitations in high-speed computing and communication systems with electronic counterparts [1]. In order to match the flexible and diverse signal processing capabilities of electronics, all-optical signal processing with high number of zeros and poles is necessary. At the same time, it is desirable that such high-order filters consist of a number of identical 'unit cells' to reduce the filter design complexity. Here, we propose and demonstrate an all-optical lattice filter [2-5] with four cascaded stages of unit cells fabricated using rib waveguides on silicon-on-insulator (SOI) platform. Such lattice filters can cover orders of magnitude wider bandwidths than electronic equivalents and avoid energy consumption at the bit rate. The optical signal processing can potentially find applications in high-speed equalization, laser radar (LADAR), electronic warfare (EW), free space optical (FSO) communications, synthetic aperture radar (SAR), electro-optic/infrared (EO/IR) sensing and many others.

**Silicon Photonic Lattice Filter Design and Unit cell performance**:

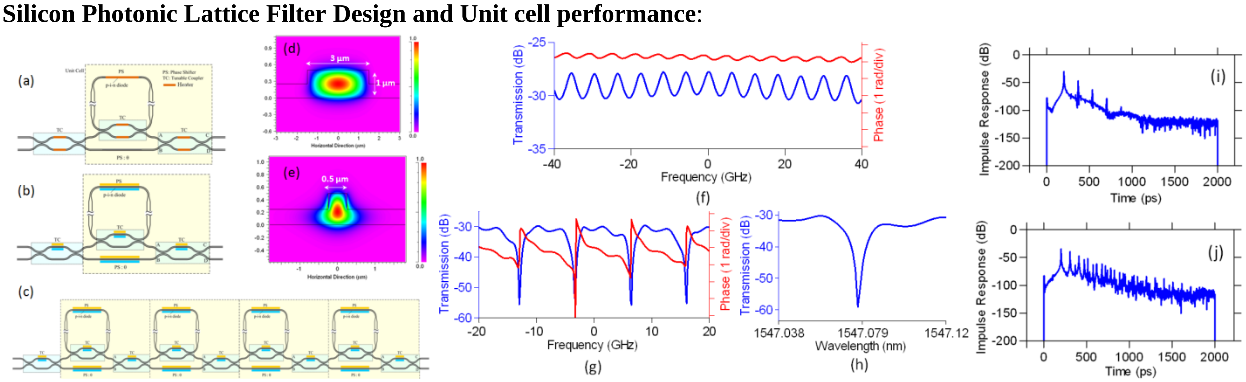


Figure 1.(a) and (b) Schematic of a single-unit-cell filter with (a) heater tuning and (b) p-i-n tuning. (c) Schematic of a four-unit-cell filter. (d)-(e) Simulated TE mode profiles of the (d) 3-µm-wide rib waveguide and (e) 0.5-µm-wide waveguide. (f)-(g) Measured transmission and phase spectra –s11 parameter– for a single-unit-cell filter with low (f) and high (g) ring coupling. (h) Zoom of single cell resonance. (i)-(j) Measured impulse response of the single-unit-cell filter corresponding to the (f) and (g) tuning conditions, respectively.

Figures 1(a) and (b) show the schematic of the device unit-cell [6], a basic building block for more complex high-order filters. The unit-cell is comprised of a Mach-Zehnder interferometer coupled with a microring resonator with several tuning elements positioned inside the cell for the reconfigurable functionality [7]. The unit cell input/output and ring couplers all consist of small tunable MZI couplers, such that the corresponding coupling coefficients can be independently controlled. Two different kinds of tuning elements have been designed, fabricated and tested. Thermo-optical tuning is achieved by integrating a nichrome (NiCr) heater above the optical waveguide section to be tuned. The heater resistance ranges from 1 to 8 kΩ corresponding to different tuning lengths. The current of the heater can be raised up to 10 mA without resulting in addition of any significant optical loss. On other hand, electrooptic tuning is obtained based on the free-carrier plasma dispersion effect in silicon by making embedded p-i-n diodes [8]. A uniform threshold current of around 0.92 mA with a DC resistance of 10 kΩ has been obtained for the different fabricated devices. The unit-cell design incorporates two types of silicon rib waveguides: a 3-µm wide waveguide to maintain low propagation loss with low optical nonlinearity and a 0.5-µm wide waveguide to allow single-mode confinement, strong lateral evanescent coupling, and low-tuning-current operation [9]. We choose to design the device using rib waveguides as they exhibit lower losses than channel waveguides. The dimensions of the waveguide are 500 nm wide, rib height of 250 nm, slab height of 250 nm, and bending radius of 300 µm. These dimension parameters ensure that the waveguide is single mode at wavelengths around 1.5 µm for the TE polarization and that the bending loss is minimized. The circumference of the racetrack resonator is 8.2 mm, giving a free spectral range of 10 GHz. The unit-cell of Fig.1(a) has an infinite impulse response due to the resonance structure [3] when the coupling coefficient between the ring resonator and the waveguide is below 1. Aa coupling coefficient value of 1 will essentially remove the resonance in the ring and make the unit-cell operate as a finite impulse response (FIR) filter. The unit-cell transfer function has one pole and one zero, determined by the tuning elements in the microring resonator, MZI-ring coupler, MZI reference arm, MZI input and output couplers. Thus, by controlling these elements, we can arbitrarily position the pole and zero within the unit circle, and realize arbitrarily reconfigurable IIR and FIR filters. Figures 1(d) and (e) show the single unit cell transmission and phase spectra after tuning the coupling coefficient to the ring resonator. By changing the current injected to two different tuning elements –one at a time– the extinction ratio of the unit cell transfer function is varied from 2 dB to 26 dB at the expense of a tuning energy of 36 mW. Figure 1(f) shows the high Q-factor of the fabricated ring estimated to be ~$10^5$.

**Silicon Photonic Lattice Filter Fabrication**:

The same design of the fully reconfigurable optical filter has been fabricated using two different sets of fabrication technology; namely the deep ultra violet (DUV) stepper-based photolithography on one hand and the electron beam (EB)-writer on the other hand. For both fabrication processes, we start with a commercial silicon-on-insulator (SOI) wafer with 3 µm of buried oxide and we make use of the photoresist reflow concept –at 145°C– to reducing the roughness transferred to the silicon waveguide during the etching step.

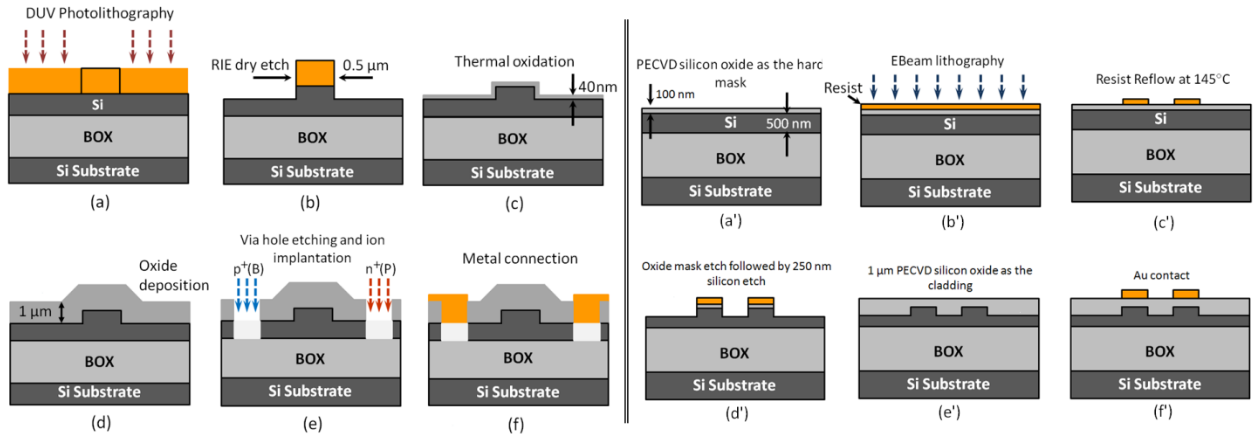

Figure 2.(a)-(f) Fabrication process flow for the CMOS compatible DUV-lithography, (a')-(f') the EB-based fabrication process flow

For the DUV-based fabrication, the mask pattern is transferred to the resist material by exposure to a laser source of 248 nm. This is followed by reactive ion etching (RIE) to form the waveguide rib, and then the oxidation of the whole wafer surface is done in two steps. First a silicon dioxide layer of 40 nm is formed by thermal oxidation before increasing the oxide thickness to 1µm through deposition. To form the embedded p-i-n diodes required for tuning, via openings are made by RIE etching then boron and phosphorus ions are implanted to form the p+ and n+ regions, respectively. The wafer is then covered by an Al layer of 600 nm and the current electrodes are formed in this Al layer by wet etching. The measured waveguide propagation losses are found to be around 0.9 dB/cm. For EB-based fabrication, we deposit 100 nm of plasma-enhanced chemical vapor deposition (PECVD) silicon oxide as the hard mask, and the device is written with e-beam lithography. The silicon rib waveguide is defined using RIE and a clad with 1 µm of PECVD silicon oxide after resist stripping to confine the optical mode. Finally, we evaporate 300 nm of nichrome above the cladding, to define the 2 µm wide microheaters which will control the device followed by making the contacts. The measured waveguide propagation losses are estimated at less than 0.5 dB/cm.

**Silicon Photonic Lattice Filter Characterization**:

The fabricated four stage cascaded lattice filters are fully characterized using optical vector network analyzer (OVNA). For the OVNA, a mode hop free swept laser signal is split into two light paths, the reference arm and the measurement setup arm containing the filter under observation. The two signals are then combined and a balanced detector is used to convert them to the electrical domain. This method retrieves complete amplitude transfer function and phase information, shown in Fig. 3.(a)-(g). The OVNA measurement apparatus used here is capable of retrieving 20 ns impulse responses with better than 1 ps temporal resolution. Figures 3(a)-(c) show the amplitude and phase of the transfer function of the four-cascaded-cell filter fabricated using the DUV photolithography. The reconfiguration currents are selected to keep the wavelength resonance location for one of the four rings clearly shifted from the others whereas optical coupling to this ring is being tuned by current change between 3.7 and 9.4 mA. Figures 3(d)-(f) show the amplitude and phase of the transfer function of the four-cascaded-cell filter fabricated using EB-writer. Different tuning currents belonging to the four cells are set to have two clear separate wavelength resonance locations in (d) then varied in (e) and (f) to increase the optical coupling to one resonance while shifting the others.

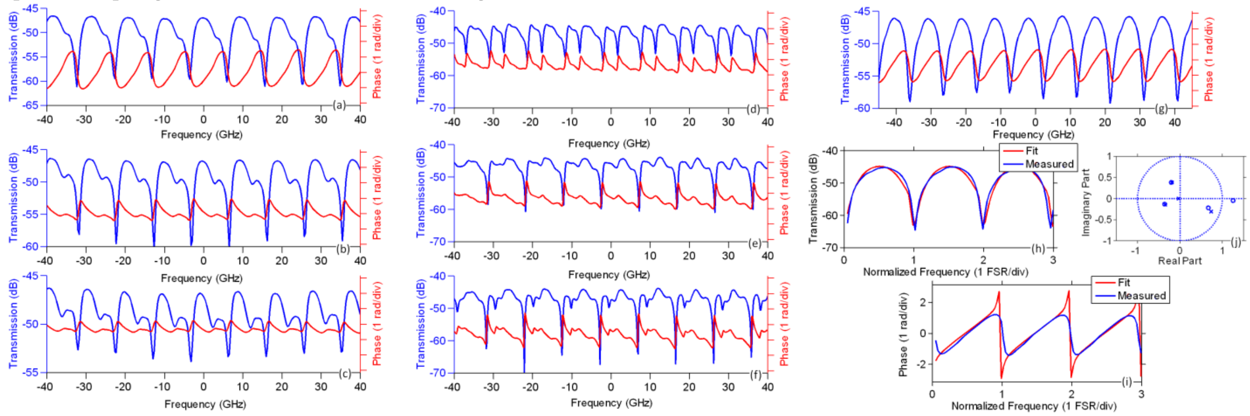


Figure 3.(a)-(c) Measured transmission and phase spectra –s11 parameter– for a DUV-based four-unit-cell filter with current tuned to change a single ring coupling. (d)-(f) Measured transmission and phase spectra –s11 parameter– for a EB-based four-unit-cell filter with current tuned to change the spectrum. (g) Measured four-unit-cell-filter spectrum and the corresponding fitted spectral (h) transmission and (i) phase using the least square method. (j) Poles ‘x’ and zeros ’o’ of the fitted transfer function.

**Silicon Photonic Lattice Filter Synthesis**:

The principal problem in filter synthesis is determining the filter parameters such that the filter transfer function matches the desired or specified one. In our case, each of the four cascaded unit cells has four tunable parameters, setting one pole and one zero. The initial values of those parameters after fabrication are unknown. The phase of the pole is designed to initially (without tuning) have zero value, but small variations in the ring’s optical path length will offset this value. Therefore, it is imperative to be able to extract actual values of the tuning parameters from the measured spectra. For a four-unit-cell filter, this is done by fourth order polynomial curve fitting to the magnitude and phase information data collected by OVNA, based on a least square approximation. For the filter transfer function shown in Fig. 2(g), the fitted amplitude and phase are given in Figs. 2(h) and (i) respectively, and the poles and zeros are plotted in Fig. 2(j). The next step is to use Jinguji’s recursion algorithm [6] to get all the tuning parameters from the polynomial function approximating the measured curve, and after current calibration versus phase change the synthesis process can be started.

**Summary**:

In summary, we have designed, fabricated, and tested a low-loss four-stage optical lattice filter unit cell on a silicon-on-insulator platform. The high-quality of the filter and the excellent fit to the theoretically predicted response allows high-order filter synthesis.

**Acknowledgement**:

This work was supported in part by DARPA MTO Si-PhASER project Grant No. HR0011-09-1-0013. L. W. Luo acknowledges a fellowship from the Agency of Science, Technology and Research (A*STAR), Singapore.

**References**:

[1] E. M. Dowling and D. L. MacFarlane, "Lightwave lattice filters for optically multiplexed communicationsystems," *Lightwave Technology, Journal of,* vol. 12, pp. 471-486, 1994.

[2] B. Moslehi, J. W. Goodman, M. Tur, and H. J. Shaw, "Fiber-optic lattice signal processing," *Proceedings of the IEEE,* vol. 72, pp. 909-930, 1984.

[3] C. K. Madsen and J. H. Zhao, *Optical filter design and analysis*: John Wiley New York, 1999.

[4] I. M. S. Panahi, G. Kannan, L. R. Hunt, D. L. MacFarlane, and J. Tong, "Lattice filter with adjustable gains and its application in optical signal processing," 2005, pp. 321-326.

[5] L. R. Hunt, V. Govindan, I. Panahi, J. Tong, G. Kannan, D. L. MacFarlane, and G. Evans, "Active optical lattice filters," *EURASIP Journal on Applied Signal Processing,* vol. 10, p. 1452, 2005.

[6] K. Jinguji, "Synthesis of coherent two-port optical delay-line circuit with ring waveguides," *Journal of Lightwave Technology*, vol. 14, pp. 1882-98, 1996.

[7] L. Zhou and A. W. Poon, "Fano resonance-based electrically reconfigurable add-drop filters in silicon microring resonator-coupled Mach-Zehnder interferometers," *Optics letters,* vol. 32, pp. 781-783, 2007.

[8] Xu, Q., Schmidt, B., Pradhan, S. and Lipson, M., Micrometre-scale silicon electro-optic modulator, Nature, Vol. 435, pp. 325-327, 19 May 2005

[9] L. Zhou, Stevan S. Djordjevic, Nicolas K. Fontaine, Zhi Ding, Katsunari Okamoto and S.J.Ben Yoo "Silicon Microring Resonator-Based Reconfigurable Optical Lattice Filter for On-Chip Optical Signal Processing " in *LEOS 2009*, 2009.